Materials Science Forum
ISSN: 1662-9752, Vol. 1183, pp 13-23
doi:10.4028/p-LDA6yf

Submitted: 2026-01-19
Revised: 2026-02-16
Accepted: 2026-02-24
Online: 2026-04-13

Microstructure Modification of Hot Formed Shafts through Customised Spray Cooling from the Forming Heat

Hammes Matthias[1,a*], Piwek Armin[1,b], Mohnfeld Norman[1,c], Peddinghaus Julius[1,d], Uhe Johanna[1,e] and Behrens Bernd-Arno[1,f]

[1]Leibniz University Hannover, Institute of Forming Technology and Machines, An der Universität 2, 30823 Garbsen, Germany

[a*]hammes@ifum.uni-hannover.de, [b]piwek@ifum.uni-hannover.de, [c]mohnfeld@ifum.uni-hannover.de, [d]peddinghaus@ifum.uni-hannover.de, [e]uhe@ifum.uni-hannover.de, [f]behrens@ifum.uni-hannover.de

*corresponding author: hammes@ifum.uni-hannover.de

Keywords: hot forming, finite element method, heat treatment, residual stresses.

Abstract. In order to achieve a long service life for highly stressed parts such as shafts for drivetrains, a combination of a bainitic microstructure with compressive surface residual stresses is beneficial. While a bainitic microstructure offers a good balance between strength and toughness, compressive residual stresses especially near the surface have a positive impact on service life. Research has shown that this is due to a shift of the crack initiation towards the core and a reduced crack growth. These properties can be achieved by hot forming as an established method for manufacturing highly stressed parts followed by an adapted cooling strategy. As this general approach was demonstrated for a simplified process in a prior study, the present article is dedicated to the functionalisation for hot forming processes. In detail, a customised spray cooling is presented for a hot impact extrusion process whereby shafts made of AISI 4140 are cooled down from the forming heat in a single step with adjusted cooling rates. In a finite element-based process design, different cooling strategies were investigated and adequate heat treatments to achieve the combined properties were identified. Following this process design, shafts are formed via hot impact extrusion and spray cooled according to the cooling strategy for experimental validation of the numerical model. Additionally, shafts with air cooling are produced as a reference. During forming, force-displacement curves are measured, which are used for the validation of the numerical hot impact extrusion simulation. The resulting plastic strain and temperature distribution significantly influence the following cooling simulation. The final microstructure as well as hardness values of the produced shafts are determined and compared for the varying cooling strategies.

Introduction

Parts manufactured via hot forming offer beneficial properties such as a finer microstructure as well as load adjusted grain orientations, leading to highly durable components [1]. In addition, a bainitic microstructure is favoured due to a good balance between strength and toughness [2], which is crucial for highly stressed parts. In order to obtain the desired mechanical properties, heat treatments are used after forming. However, these treatments influence the residual stresses on the surface, where often tensile stresses remain which have a negative impact on service life. On the other hand, compressive residual stresses positively influence crack initiation and propagation leading to later component failure and longer service life [3].

Residual stresses form due to different reasons: plastic deformation, local unequal thermal contraction of the surface and the core or changes in the microstructure [4]. Furthermore, these stresses are present while no external loads are applied. In this context, the formation of martensite is relevant, since due to the diffusionless transformation of martensite, a highly strained tetragonal crystal structure forms leading to an increase in volume. In turn, this increase in volume leads to compressive residual stresses [4]. Therefore, martensite formation is linked with compressive residual

stresses, and a combination of martensite near the surface and bainite in the core is desired, which is the aim of this process design through numerical studies.

When modelling the behaviour of the different microstructures of steel, phase-specific properties are required. In most cases, it is difficult to generate experimental material data for pure microstructural phases. However, these properties can also be calculated based on the chemical composition and empirical equations founded on physical principles as an estimation, which can be used instead [5].

The benefit of heat treatments directly from the forming heat are shown in [6, 7], where tailor-made cooling strategies involving spray cooling led to adapted component properties. In order to implement the spray cooling process in simulations, heat transfer coefficients (HTC) are needed. These are determined with an experimental-numerical approach, where cooling curves are measured and the experimental setup subsequently simulated, adjusting the HTC values until the cooling curves of the simulation and the experiment match [8]. Through spray cooling, different cooling rates can be realised between the surface and the core, leading to an adapted microstructure.

When combining heat treatment and surface residual stress modification in one step, energy and resources can be saved compared to the conventional production route consisting of separate production steps since no reheating is necessary. Previous studies with simple cylindrical specimens showed that compressive residual stresses can be induced directly after hot upsetting with an adapted cooling strategy. The investigated steel was AISI 52100, with the focus on the formation of pearlite and martensite regarding the microstructure [9]. However, this research is dedicated to the manufacturing of shafts made of AISI 4140 via hot impact extrusion. The shafts are immediately cooled from the forming heat in order to achieve different microstructures consisting of bainite and martensite. The focus of this paper lies on the experimental validation of the implemented material models used for the process design with numerical simulations. A validated simulation model, especially regarding the prediction of the microstructure after forming and cooling, is essential for the prediction and further optimisation of residual stresses.

Materials and Methods

The semi-finished products in this study were cylindrical steel bars made of AISI 4140 with a diameter of 30 mm and a length of 130 mm. The general process route is shown in Fig. 1, which consists of three major steps: Heating and homogenous austenitisation of the semi-finished product at 1,150 °C, followed by a hot impact extrusion operation and a subsequent adapted cooling from the forming heat.

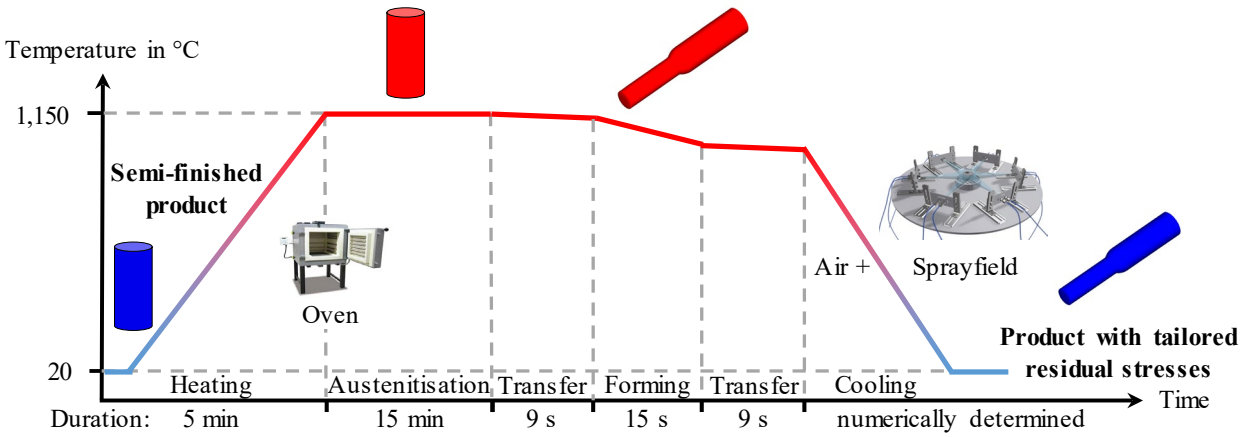

Fig. 1. General process route of the hot formed shafts with subsequent cooling.

At first, the influence of different cooling strategies on the resulting surface residual stresses were investigated in pre-studies with finite element (FE) simulations in Simufact forming v2025.2. For the hot impact extrusion, both punch and die are modelled as rigid heat-conducting dies made of tool steel AISI M2. The values for the specific heat capacity and the thermal conductivity were taken from

the Simufact forming material library. Friction was modelled by a combined Coulomb-Tresca model with a friction coefficient of 0.3 [10] and a friction shear factor of 0.4 [11]. In addition, a constant HTC of 20 kW/(m²·K) between the workpiece and the dies was implemented [12]. For the calculation of flow curves of AISI 4140, the GMT model specified in Eq. 1 was calibrated with experimental cylinder compression tests [13].

$$k_f = c_1 \cdot e^{c_2 \cdot T} \cdot \varepsilon^{n_1 \cdot T + n_2} \cdot e^{\frac{l_1 \cdot T + l_2}{\varphi}} \cdot \dot{\varepsilon}^{m_1 \cdot T + m_2} \quad (1)$$

The flow stress k_f is calculated as a function of the true strain ε, the true strain rate $\dot{\varepsilon}$ and temperature T with the material specific coefficients given in Table 1.

Table 1. Fitted GMT model parameters [13].

c_1 in MPa·s	c_2 in $\frac{1}{°C}$	n_1 in $\frac{1}{10^{5} \cdot °C}$	n_2 in -	l_1 in $\frac{1}{10^{5} \cdot °C}$	l_2 in -	m_1 in $\frac{1}{10^{5} \cdot °C}$	m_2 in -
6054.21	-0.0039	-3.0846	0.3000	1.8926	-0.03548	-9.4422	0.2484

In addition, time-temperature-transformation diagrams are implemented for AISI 4140, which were experimentally determined in [14], as the final phase distribution is of high interest. Furthermore, phase changes play an important role in the evolution of residual stresses. The transformation induced plasticity (TRIP) effect is also taken into account by implementing phase-specific TRIP-coefficients, evaluated with an experimental-numerical approach in [14]. The remaining material parameters for each phase were calculated with the software JMatPro, which uses the chemical composition of the alloy and empirical equations. Therefore, temperature-dependent and phase specific values were obtained for the specific heat capacity, thermal conductivity, thermal expansion coefficient, density, Young's modulus, Poisson's ratio, latent heat and hardness of AISI 4140. In addition, the flow curves were revaluated for each phase. The total strain is calculated with the additive strain decomposition method from the implicit MSC.Marc solver, where the total strain is calculated as the sum of the elastic and plastic strain increments as well as the thermal, transformation-induced and transformation-plasticity strain increments [14].

For both the forming and cooling simulations, a 2D-FE model was developed due to the rotational symmetry of the process, as shown in Fig. 2.

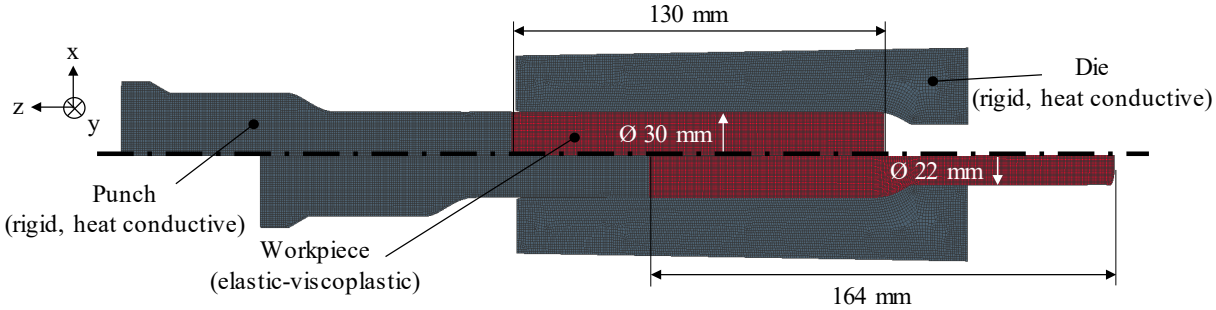

General parameters
Spindle press kinematic, 51 mm stroke
2D rotational symmetric model, Implicit MSC.Marc solver

Tool parameters
4-node quadrilateral elements (element no. 40), element edge length: 0.75 mm
Initial temperature: 20 °C | Combined friction model (μ = 0.3 | m = 0.4)

Workpiece parameters
4-node quadrilateral elements (element no. 10), element edge length: 0.5 mm
Initial temperature: 1150 °C | Initial microstructure: 100% austenite

Fig. 2. FE model of hot impact extrusion, top: before forming, bottom: after forming.

An element edge length of 0.5 mm was chosen for the workpiece following a mesh sensitivity study, offering a good trade-off between result accuracy and computation time. The initial condition implemented for the forming simulation consists of a numerically calculated thermally expanded cylindrical billet with a temperature of 1,150 °C and a 100% austenitic microstructure for the initial process design. In addition, an impact velocity of 500 mm/s was defined, in accordance with the experimental setup. The workpiece is extruded to a diameter of 22 mm with a stroke of 51 mm. Subsequently, the geometry as well as the stress and temperature field were transferred to a cooling simulation. A combination of air and spray cooling is investigated by implementing temperature-dependent surface HTC. The HTC were determined with an experimental-numerical approach, as detailed in [15]. The spray was mixed in the nozzle with a water pressure of 0.04 MPa and an air pressure of 0.1 MPa. Fig. 3 shows the implemented HTC curves.

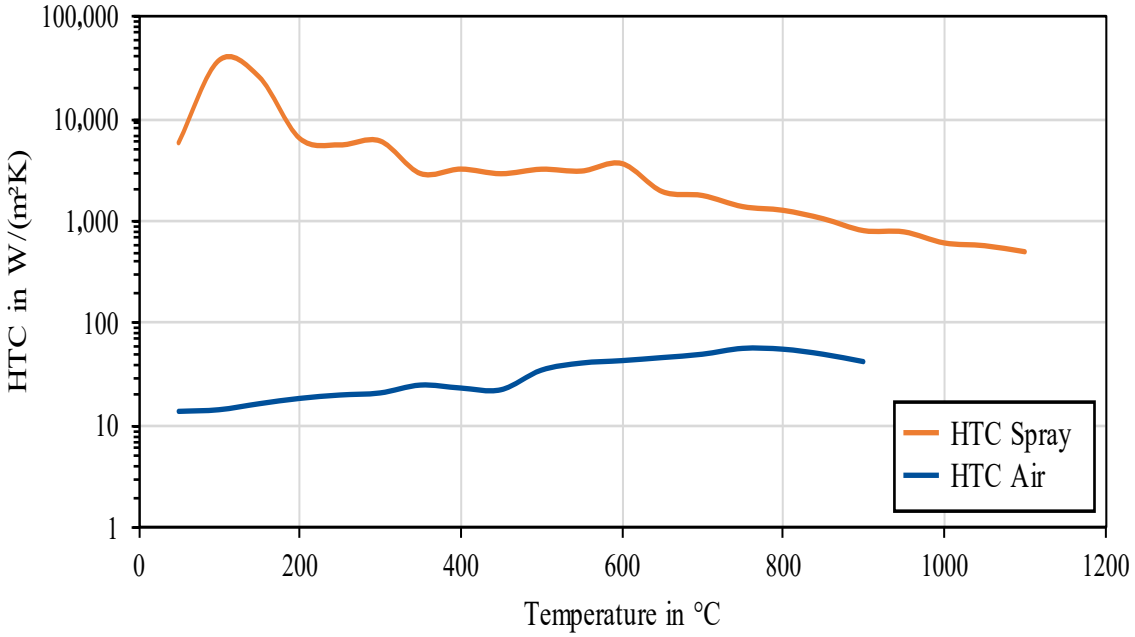

Fig. 3. HTC depending on the temperature between air or spray and AISI 4140 steel based on [15].

The plot shows high HTC values for the spray, with a peak of approximately 37 kW/m^{2}K at 100 °C, whereas the values for air are in a much lower range, with a maximum of 60 W/m^{2}K at 750 °C. Overall, the spray cooling behaviour can be separated in three different stages, starting with film boiling at high temperatures and lower HTC, leading to nucleate boiling at lower temperatures with very high HTC, which drop rapidly due to the change to convection with falling temperature. In contrast, air cooling exhibits only free convection. In order to precisely assign the specific HTC for spray cooling to a defined surface, the near-field contact function of Simufact Forming was used. For the remaining surfaces not exposed to the spray, the HTC between steel and air was assigned.

For the experimental validation, the workpiece was heated to 1,150 °C and held for 15 min for full austenitisation under argon gas atmosphere in order to reduce scaling. Afterwards, the workpiece was manually transferred in approximately 9 s to the spindle press Lasco SPR 500 for impact extrusion. Before each extrusion, the die was manually lubricated with an oil-based lubricant (Berulit 722, Bechem). The punch was fitted with strain gauges, allowing for direct force measurements without the influence of the machine stiffness. The corresponding displacement was given by the machine control. Fig. 4.a) shows the experimental setup.

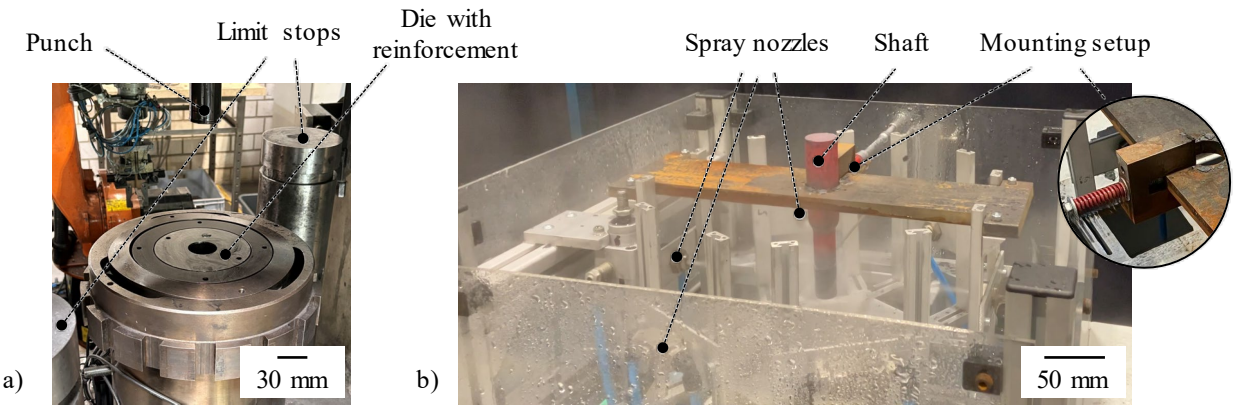

Fig. 4. a) Press space of the Lasco SPR 500 spindle press with installed tools and b) spray cooling station.

Following the ejection of the formed shaft, it was transferred manually in approximately 9 s to the cooling station. It was mounted near the top of the greater diameter with the smaller diameter pointing downwards. This allows only the smaller section and the shoulder area to be cooled by the spray. The cooling station and the mounting setup for the extruded shaft are shown in Fig. 4.b). Six nozzles were placed in a circular pattern in order to ensure uniform cooling from all sides.
During initial testing of the experimental setup, it was found that the temperature loss after transfer to the cooling station was higher compared to the initial simulation due to the clamping setup. In order to measure the differing cooling behaviour, a near-surface temperature-time measurement was conducted with an already formed shaft, which was reheated in the oven for 15 min for full austenitisation and then mounted in the cooling station where no spray cooling was used. Direct surface measurements by contacting the surface with a type K thermocouple proved unsuccessful, since the measured temperature was too low due to scaling.

Consequently, in order to generate different ratios of martensite, two cooling routes were experimentally investigated with five extruded shafts each, differing in starting times of the spray cooling as well as spray cooling durations, based on the near-surface temperature-time measurement and numerical pre-studies. Table 2 gives an overview of the different cooling sequences.

Table 2. Cooling sequences for different strategies.

	Strategy 1	Strategy 2
1. Air cooling for	380 s	340 s
2. Spray cooling for	4 s	9 s
3. Air cooling for	136 s	140 s
4. Spray cooling for	120 s	150 s
5. Air cooling	until the whole shaft reaches room temperature	

All the aforementioned parameters were also used for the simulation of the whole experimental process chain including transfers.

For the analysis of the microstructure and the hardness measurements, the shafts were cut in half lengthwise and samples were taken from the transition area. The etchant used was 2% alcoholic nitric acid (nital), and for the micro hardness measurement Vickers-indents (HV0.1) were utilised.

Results and Discussion

For a validation of the forming step, the numerical force-displacement curves were compared to the experimental results, shown in Fig. 5.

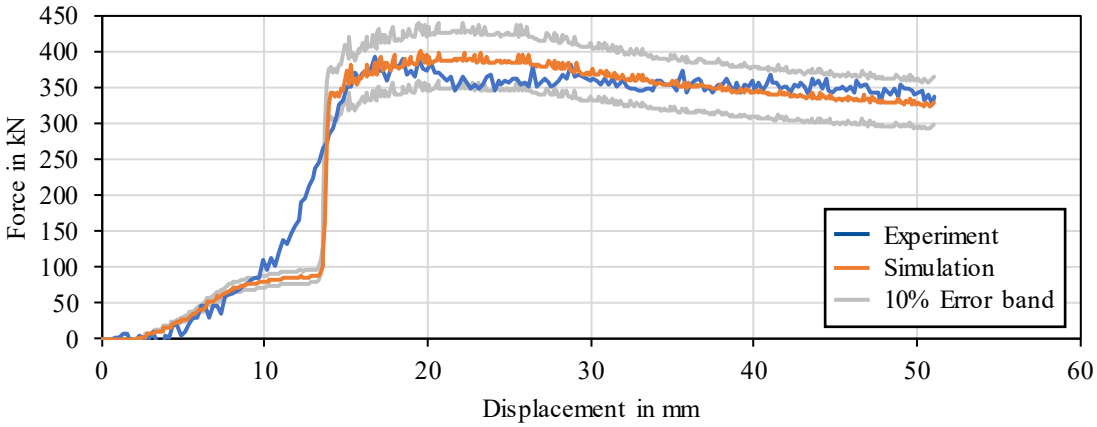

Fig. 5. Experimentally and numerically determined force-displacement curves of hot impact extrusion.

The numerical results show a good agreement with the experimental data, with only minor differences in the increase of force. During experiments, a smoother increase can be seen due to a higher contact area between the workpiece and the slightly greater forming die. This results from an eccentrical insertion leading to unsymmetrical bulging, which in turn increases the contact area steadily, whereas in the simulation, a perfect centred position is implemented. Here, the deformation occurs mainly in the tapered zone of the forming die, leading to a steady increase in force at first. At the same time, the initial cylinder outside the main forming zone increases until the surface comes into contact with the slightly greater forming die resulting in instant additional friction, which is seen in a sharp force increase. Starting from the maximum force, which is around 400 kN in both curves, is the relevant part for the forming process, where a good agreement is desired. The slope following the force peak is slightly steeper in the simulation compared to the experimental results, since during experiments the friction conditions change with decreasing friction surface, while in the simulation the conditions do not change, but the surface decreases resulting in lower forces. Overall, the maximum difference between experimental and numerical results after the initial force peak does not exceed 10%, which indicates an adequate model with suitable assumed boundary conditions such as friction [16].

For the cooling simulation, a numerical pre-study was conducted in order to identify suitable cooling strategies leading to significant compressive surface residual stresses as well as a mainly bainitic microstructure (see Fig. 6).

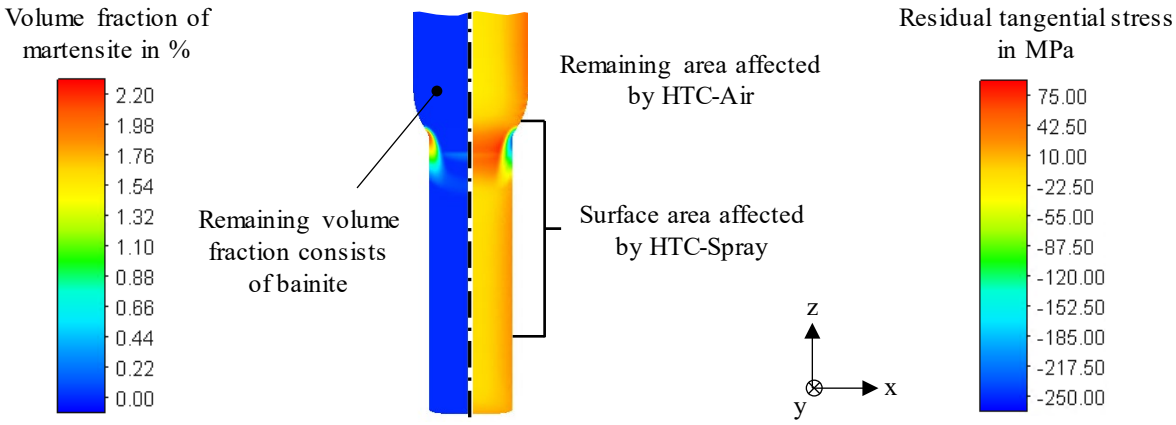

Fig. 6. Residual tangential stress and martensite distribution after initial process design.

The results show that a small formation of martensite can lead to compressive surface residual stresses, formed at the transition section between the smaller diameter and the shoulder, where the highest stresses are present in later usage due to the geometric discontinuity. The corresponding cooling strategy involved air cooling for approximately 11 min, followed by spray cooling for 3 s and

a spray cooling pause for 110 s until spray cooling is resumed. The spray cooling pause was set in order to allow bainite transformation in the core, resulting in martensite formation only near the surface. Further numerical pre-studies were conducted for different amounts of martensite. Based on these pre-studies and the temperature-time measurement of the reheated shaft, the cooling sequences shown in Table 2 were adapted.

For the simulation of the whole experimental process chain, the HTC of the mounting setup was determined similar to the air and spray behaviour and implemented in the model. The resulting microstructure of the numerical calculation is compared to the experiments using micrographs as well as hardness measurements for validation. Strategy 1, where spray cooling starts after 380 s, shows a mixed microstructure in the numerical simulation consisting of bainite with a maximum volume fraction of 68% near the surface and martensite with a maximum volume fraction of 39% near the core (see Fig. 7).

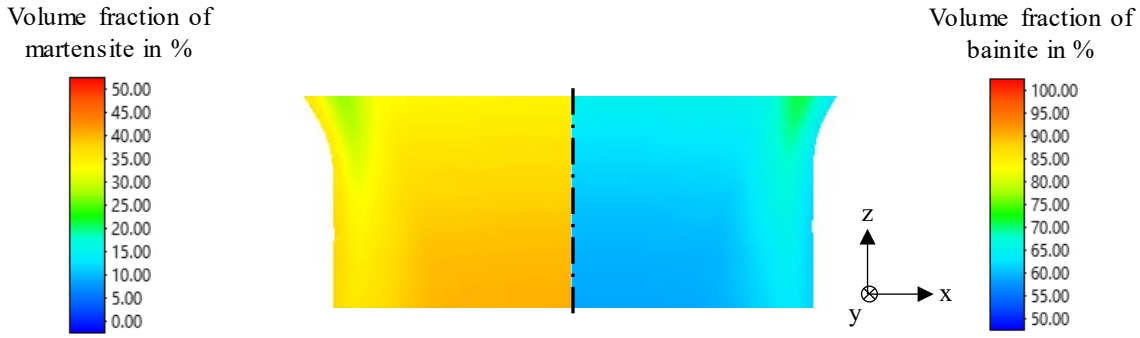

Fig. 7. Mixed microstructure from numerical simulation of strategy 1.

The results show that the mounting setup has a major influence on the whole thermal behaviour of the system, which leads to a significant amount of martensite near the core. In the corresponding micrograph shown in Fig. 8.a), a mixed microstructure of bainite and martensite is also present.

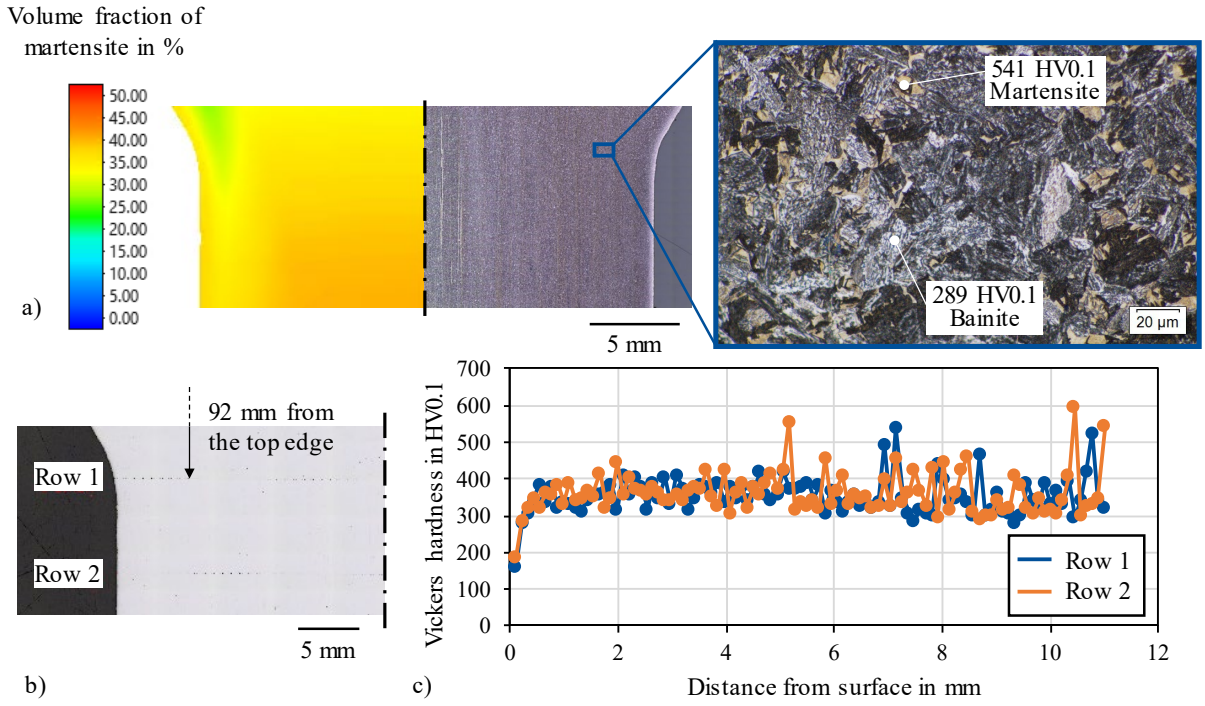

Fig. 8. a) Comparison between numerical (left) and experimental microstructure with hardness values of the individual phases (right) and b) location of hardness profile measurements and c) hardness profiles for both rows for strategy 1.

The harder phase of 541 HV0.1 corresponds to martensite, while the softer of 289 HV0.1 is bainite. These individual measurements were taken from hardness profiles, where only a single phase was indented, and the hardness profiles were measured in two rows approximately 4 mm apart (see Fig. 8.b)). Regarding the measurements shown in Fig. 8.c), the hardness profile shows fluctuations through the core, indicating a finely distributed microstructure with an increasing amount of martensite. The first indents close to the surface have a lower hardness due to a slightly lower martensite fraction as well as a coarser grained bainitic ferrite which is mostly indented. Following the rule of mixtures, the measured mixed hardness can be interpreted as the sum of the hardness of the individual phases taken from single-phase indentations, weighted with their respective volume fraction [17]. Therefore, the average hardness of 356 HV0.1 for row 1 and 364 HV0.1 for row 2 indicate a ratio of approximately 70% bainite and 30% martensite, which also agrees with [18], where Vickers hardness values were determined for different microstructures of bainite and martensite of the same AISI 4140 steel. Compared to the simulation, the calculated ratios are in a similar range, but with small deviations.

Starting the spray cooling earlier as in strategy 1 results in an increase of martensite formation as seen in Fig. 9.a).

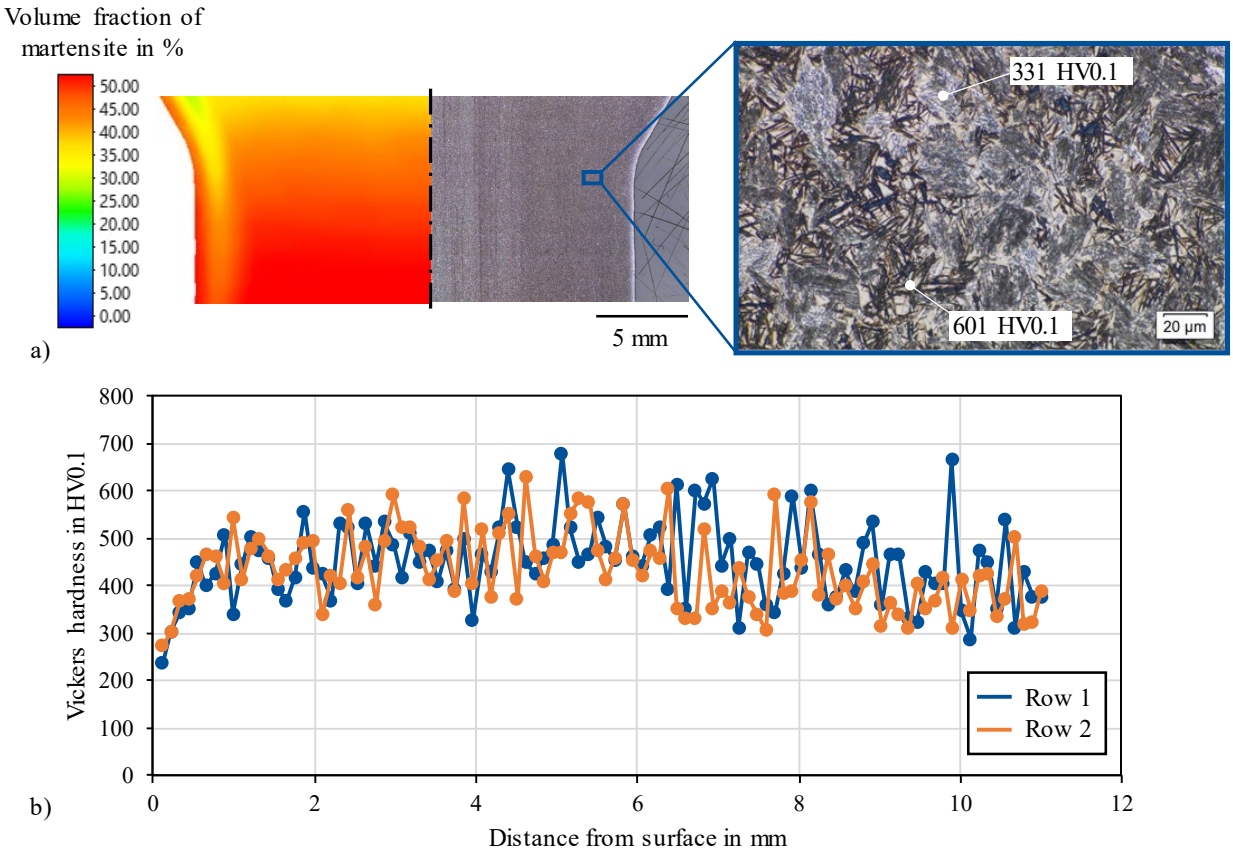

Fig. 9. a) Comparison between numerical (left) and experimental microstructure with hardness values of the individual phases (right) and b) hardness profiles for both rows for strategy 2.

The micrograph shows a fine microstructure with a higher amount of martensite compared to strategy 1, which is also seen in the high fluctuations of the hardness measurements in Fig. 9.b). An average hardness of 450 HV0.1 for row 1 and 432 HV0.1 for row 2 corresponds to around 58% bainite and 42% martensite. The simulation yields values of up to 45% martensite.

Overall, it can be seen in both strategies that due to the mounting setup, the thermal behaviour of the system was greatly changed, leading to the formation of significant amounts of martensite near the core. This also results in different residual stresses on the surface of the shaft predicted by the adjusted simulation considering the thermal influence of the mounting. Fig. 10 shows the comparison of the final microstructures between experiment and simulation for the two strategies.

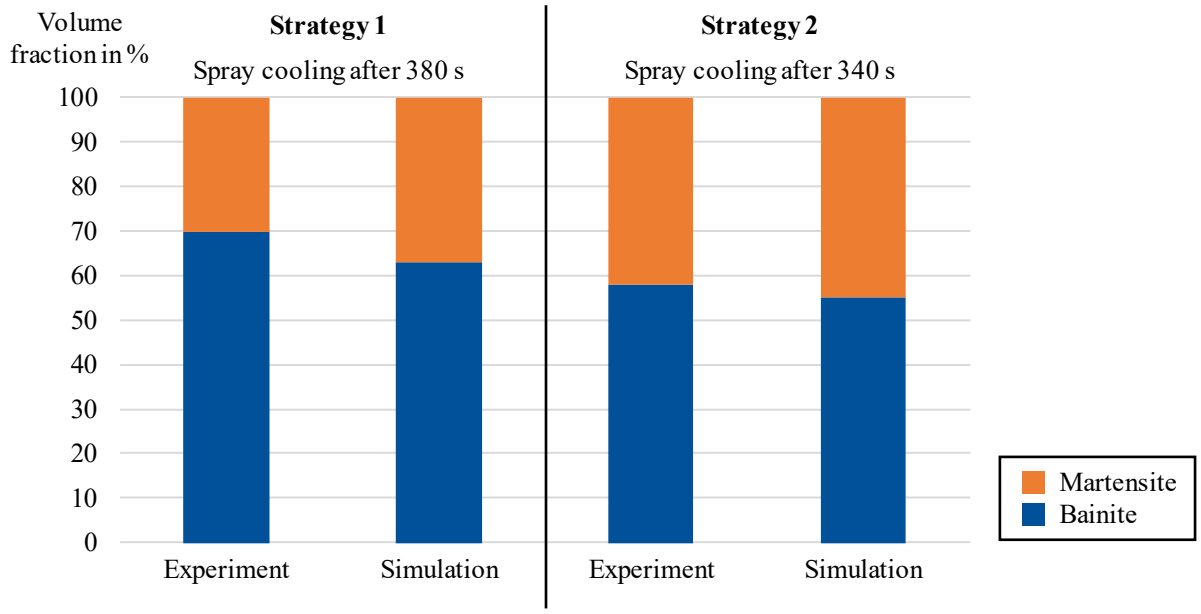

Fig. 10. Comparison of final microstructures between experiment (derived from hardness values) and simulation for the two strategies.

Generally, the simulation shows a slight overestimation of the martensite fraction. For the characterisation of the spray cooling behaviour, the resulting HTC implemented in the simulation were determined with small cylindrical specimens, where the whole cylinder surface was directly sprayed on. In contrast, the surface of the shafts is only partially sprayed, where excess water drips down towards the tip leading to a slightly different cooling performance, thus resulting in the aforementioned difference.

Summary and Outlook

For the validation of the numerical models regarding forming and cooling, the process chain was experimentally realised. By comparing the force-displacement curves of the numerical model and the experiment, a good agreement was found, validating the forming simulation. In addition, two different cooling routes were investigated and the resulting microstructures of simulation and experiment were compared. Here, also a good agreement was found for both strategies. In strategy 1, 30% martensite forms, while the simulation predicts 37%. When comparing strategy 2, 42% martensite was determined in the experimental microstructure, where the simulation shows 45%. However, it can be seen that the martensite formation was not only close to the surface but also in the core in both strategies due to the change of heat transfer caused by the mounting setup. Therefore, the mounting setup for the shafts in the cooling station has to be modified in future work, so that the contact between specimen and mount is reduced to a minimum. In addition, the HTC of the spray should be determined where the surface is only partially sprayed and compared to the initial results with full surface spray. Furthermore, the cooling strategy has to be optimised by numerical process design in order to find the optimal cooling parameters so that a predominantly bainitic microstructure forms in the core. Additionally, the induced surface residual stresses of the experimentally formed shafts are to be measured and compared to the numerical results.

Acknowledgement

This research was funded by the Deutsche Forschungsgemeinschaft (DFG, German Research Foundation) – project number 530125423.

References

[1] J. A. Suris, C. C. Yurgel, R. Alves de Sousa, Influence of the Grain-Flow Orientation after Hot Forging Process Evaluated through Rotational Flexing Fatigue Test, Metals 13-2 (2023) 187, doi: 10.3390/met13020187.

[2] H. K. D. H. Bhadeshia, Bainite in steels: Theory and practice, third ed., Maney Publishing, Leeds/London, 2015.

[3] A. Wildeis, H.-J. Christ, R. Brandt, Influence of Residual Stresses on the Crack Initiation and Short Crack Propagation in a Martensitic Spring Steel, Metals 12-7 (2022) 1085, doi: 10.3390/met12071085.

[4] K. Palaniradja, N. Alagumurthi, V. Soundararajan, Residual Stresses in Case Hardened Materials, The Open Materials Science Journal 4-1 (2010) 92–102, doi: 10.2174/1874088X010040300092.

[5] N. Saunders, U. K. Z. Guo, X. Li, A. P. Miodownik, J.-P. Schillé, Using JMatPro to model materials properties and behavior, Journal of the Minerals, Metals & Materials Society 55-12 (2003) 60–65, doi: 10.1007/s11837-003-0013-2.

[6] T. Gretzki, C. Krause, I. Frolov, T. Hassel, M. Nicolaus, F.-W. Bach, M. Kästner, O. Abo-Namous, E. Reithmeier, Manufacturing Surface Hardened Components of 42CrMo4 by Water-Air Spray Cooling, Steel Research Int. 80-12 (2009) 906–915, doi: 10.2374/SRI09SP131.

[7] D. Rodman, C. Krause, F. Nürnberger, F.-W. Bach, K. Haskamp, M. Kästner, E. Reithmeier, Induction Hardening of Spur Gearwheels Made from 42CrMo4 Hardening and Tempering Steel by Employing Spray Cooling, Steel Research Int. 82-4 (2011) 329–336, doi: 10.1002/srin.201000218.

[8] H. S. Hasan, M. J. Peet, J. M. Jalil, H. K. D. H. Bhadeshia, Heat transfer coefficients during quenching of steels, Heat Mass Transfer 47-3 (2011) 315–321, doi: 10.1007/s00231-010-0721-4.

[9] B.-A. Behrens, K. Brunotte, H. Wester, C. Kock, Targeted adjustment of residual stresses in hot-formed components by means of process design based on finite element simulation, Arch. Appl. Mech. 91-8 (2021) 3579–3602, doi: 10.1007/s00419-021-01928-y.

[10] I. Serebriakov, E. S. Puchi-Cabrera, L. Dubar, P. Moreau, D. Meresse, J. G. La Barbera-Sosa, Friction analysis during deformation of steels under hot-working conditions, Tribology International 158 (2021) 106928, doi: 10.1016/j.triboint.2021.106928.

[11] D. Jeong, D. Kim, J. Kim, B. Kim, T. Dean, Effects of surface treatments and lubricants for warm forging die life, Journal of Materials Processing Technology 113-1-3 (2001) 544–550, doi: 10.1016/S0924-0136(01)00693-8.

[12] P. R. Burte, Y.-T. Im, T. Altan, S. L. Semiatin, Measurement and Analysis of Heat Transfer and Friction During Hot Forging, Journal of Engineering for Industry 112-4 (1990) 332–339, 1990, doi: 10.1115/1.2899596.

[13] B.-A. Behrens, J. Schröder, H. Wester, D. Brands, S. Uebing, C. Kock, Experimental and Numerical Investigations on the Development and Stability of Residual Stresses Arising from Hot Forming Processes, in: G. Daehn, J. Cao, B. Kinsey, E. Tekkaya, A. Vivek, and Y. Yoshida (Eds.), Forming the Future (The Minerals, Metals & Materials Series), Springer International Publishing, Cham, 2021, pp. 2289–2301.

[14] B.-A. Behrens, A. Chugreev, C. Kock, Macroscopic FE-Simulation of residual stresses in thermo-mechanically processed steels considering phase transformation effects, in: E. Oñate, D.R.J. Owen, D. Peric M. Chiumenti, and E. de Souza Neto, (Eds.), XIV International Conference on Computational Plasticity: Fundamentals and Applications (COMPLAS 2019), Barcelona, 2019.

[15] B.-A. Behrens, J. Schröder, D. Brands, L. Scheunemann, R. Niekamp, A. Chugreev, M. Sarhil, S. Uebing, C. Kock, Experimental and Numerical Investigations of the Development of Residual Stresses in Thermo-Mechanically Processed Cr-Alloyed Steel 1.3505, Metals 9-4 (2019) 480, doi: 10.3390/met9040480.

[16] Z. Keran, M. Math, P. Piljek, FEM Analyses of Friction Coefficient in Open Die Coining Process of Different Grain Sizes, Journal Material Sci. & Eng. 1-1 (2012) 5, doi: 10.4172/2169-0022.1000105.

[17] M. Alibeyki, H. Mirzadeh, M. Najafi, A. Kalhor, Modification of Rule of Mixtures for Estimation of the Mechanical Properties of Dual-Phase Steels, Journal of Material Eng. and Perform. 26-6 (2017) 2683–2688, doi: 10.1007/s11665-017-2687-6.

[18] F. Nürnberger, O. Grydin, M. Schaper, F.-W. Bach, B. Koczurkiewicz, A. Milenin, Microstructure Transformations in Tempering Steels during Continuous Cooling from Hot Forging Temperatures, Steel research int. 81-4 (2010) 224–233, doi: 10.1002/srin.200900132.

The publication of this article was funded by the Leibniz Universität Hannover (LUH) / Technische Informationsbibliothek (TIB)